Journal of the Mechanical Behavior of Biomedical Materials 79 (2018) 53–63

Contents lists available at ScienceDirect

Journal of the Mechanical Behavior of Biomedical Materials

journal homepage: www.elsevier.com/locate/jmbbm

In vitro biomechanical and hydrodynamic characterisation of decellularised human pulmonary and aortic roots

A. Desai[a], T. Vafaee[a], P. Rooney[b], JN. Kearney[b], HE. Berry[a,c], E. Ingham[a], J. Fisher[a], LM. Jennings[a,*]

[a] Institute of Medical and Biological Engineering, Faculties of Engineering & Biological Sciences, University of Leeds, Leeds LS2 9JT, UK
[b] NHS Blood and Transplant Tissue & Eye Services, Speke, Liverpool L24 8RB, UK
[c] Tissue Regenix Ltd., Swillington, Leeds LS26 8XT, UK

ARTICLE INFO

Keywords:
Aortic valve
Pulmonary valve
Decellularisation
Hydrodynamic function
Biomechanics

ABSTRACT

Background and purpose of the study: The use of decellularised biological heart valves in the replacement of damaged heart valves offers a promising solution to reduce the degradation issues associated with existing cryopreserved allografts. The purpose of this study was to assess the effect of low concentration sodium dodecyl sulphate decellularisation on the in vitro biomechanical and hydrodynamic properties of cryopreserved human aortic and pulmonary roots.

Method: The biomechanical and hydrodynamic properties of cryopreserved decellularised human aortic and pulmonary roots were fully characterised and compared to cellular human aortic and pulmonary roots in an unpaired study. Following review of these results, a further study was performed to investigate the influence of a specific processing step during the decellularisation protocol ('scraping') in a paired comparison, and to improve the method of the closed valve competency test by incorporating a more physiological boundary condition.

Results: The majority of the biomechanical and hydrodynamic characteristics of the decellularised aortic and pulmonary roots were similar compared to their cellular counterparts. However, several differences were noted, particularly in the functional biomechanical parameters of the pulmonary roots. However, in the subsequent paired comparison of pulmonary roots with and without decellularisation, and when a more appropriate physiological test model was used, the functional biomechanical parameters for the decellularised pulmonary roots were similar to the cellular roots.

Conclusion: Overall, the results demonstrated that the decellularised roots would be a potential choice for clinical application in heart valve replacement.

1. Introduction

For several decades, severely damaged heart valves have been treated by replacement valve surgery (Maganti et al., 2010). Although current mechanical and biological heart valve replacements improve patient survival and quality of life, problems such as thrombosis, infection and limited durability still occur and none of the current conventional valve replacements has the capacity to grow in young patients (Alpert and Dalen, 1987; Roudaut et al., 2007; Kidane et al., 2009). For young patients under the age of 18 years with severe aortic heart valve disease, the Ross procedure using a pulmonary autograft is the preferred replacement valve substitute (Alsoufi et al., 2009). A cryopreserved pulmonary allograft is then implanted in the right ventricular outflow tract (RVOT), although these have limitations including variability in their durability. Failure typically occurs due to calcification of the valve, driven by chronic inflammation and immune rejection resulting in valvular stenosis or insufficiency (Hawkins et al., 2000; Shaddy and Hawkins, 2002; Wells et al., 2002). The immune response is thought to be provoked by the presence of antigenic cells within the implanted tissue (Dignan et al., 2003; Ryan et al., 2006). Therefore, efficient decellularisation to remove the cells should reduce the host response to heart valve allografts. Previous clinical studies of decellularised human heart valves have shown favourable initial in vivo results (Elkins et al., 2001; Cebotari et al., 2006; da Costa et al., 2010; Dohmen, 2012).

During each cardiac cycle, cellular human heart valves are continuously subjected to mechanical and fluid induced stresses (Sacks and Yoganathan, 2007). Therefore, replacement heart valves should have enough strength to continuously withstand pressure and flow rates comparable to those they will experience in the human body.

* Corresponding author.
E-mail address: l.m.jennings@leeds.ac.uk (L. Jennings).

https://doi.org/10.1016/j.jmbbm.2017.09.019
Received 4 September 2017; Accepted 12 September 2017
Available online 14 September 2017

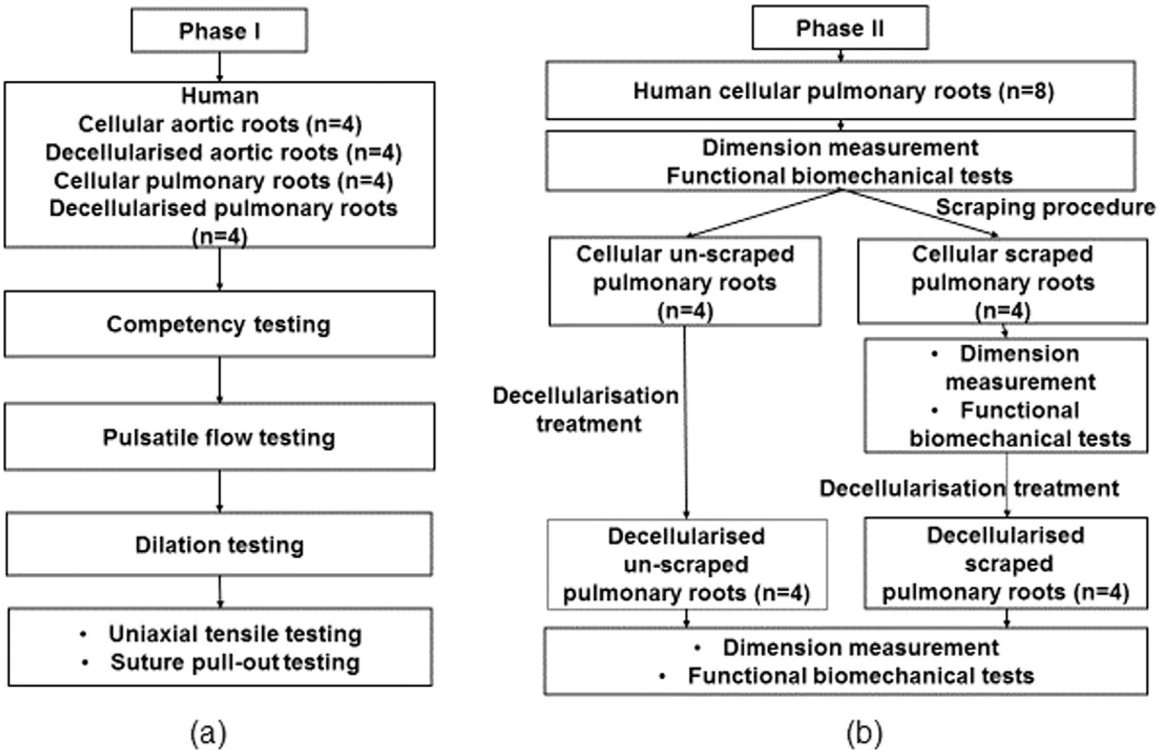

Fig. 1. Flow chart depicting the sequence of events used in (a) Phase I and (b) Phase II of the study in which functional biomechanical tests included competency testing (with and without annulus support) and dilation testing.

Decellularisation is the process of removing all the cellular components from biological tissue, leaving the extracellular matrix (ECM) intact, which can then potentially be reseeded with new progenitor cells or composites (Sacks et al., 2009a). Numerous types of detergents and biological agents have been used for decellularisation with varying concentrations, including SDS (Booth et al., 2002; Luo et al., 2014), trypsin (Liao et al., 2008), EDTA (Liao et al., 2008; Paniagua Gutierrez et al., 2015), Triton X-100 (Liao et al., 2008) (Jordan et al., 2012) and hypertonic solutions (Jordan et al., 2012). It has previously been reported that decellularisation treatment can introduce changes in the tissue structure, which may influence the mechanical properties of the tissue (Korossis et al., 2002; Spina et al., 2003; Gilbert et al., 2006). Therefore, to determine whether decellularised valves are suitable for clinical use, it is important to thoroughly assess functional performance including both the mechanical properties of the decellularised tissue and investigation of the performance of the decellularised valve under physiological flow conditions. Various test methods have been used to assess both the mechanical properties of valve tissue such as flexural (Engelmayr et al., 2005; Sacks et al., 2009b), local indentation (Cox et al., 2006), biaxial tensile (Sacks et al., 2009b; Billiar and Sacks, 2000; Fisher et al., 1986), uniaxial tensile (Luo et al., 2014; Korossis et al., 2002; Anssari-Benam et al., 2011), suture pull-out (Edwards et al., 2005; Walraevens et al., 2008), and dilation (Jennings et al., 2002; Korossis et al., 2005) as well as hydrodynamic performance of the valves under physiological flow conditions (Fisher et al., 1986; Jennings et al., 2002; Syedain et al., 2013; Reimer et al., 2015).

A number of studies have investigated the effects of decellularisation on in vitro biomechanical and hydrodynamic properties of xenogeneic heart valves (Luo et al., 2014; Korossis et al., 2002; Schenke-Layland et al., 2003; Lichtenberg et al., 2006; Tudorache et al., 2007). The results from these studies are varied due to differences in the species, decellularisation protocol, test conditions and testing methodologies. However, there has been only one study (Elkins et al., 2001) which compared in vitro hydrodynamic and biomechanical properties of cellular and decellularised human pulmonary heart valves to determine the effect of decellularisation on the properties of the tissue. In this study, the roots were tested under pulsatile flow conditions and mechanically using uniaxial tensile and suture retention test protocols. No differences in biomechanical and hydrodynamic properties were detected between the cellular and decellularised roots. However, the lack of information on the test conditions used in the biomechanical tests and limited quantitative results presented (Elkins et al., 2001) limit critical analysis of this study.

A limited number of studies (Courtman et al., 1994; Rieder et al., 2004) have used a high concentration of SDS for complete decellularisation of tissue. These studies have indicated that high concentration SDS decellularisation may induce changes in the mechanical properties of the tissue, as SDS can alter protein-protein interactions by opening the molecular structure of elastin and disturbing the bonding of collagen. Whereas, low concentration SDS based decellularisation treatment has shown favourable results for porcine aortic and pulmonary valves (Luo et al., 2014; Wilcox et al., 2005). Therefore, it was hypothesised that the low concentration SDS based treatment would minimally affect or maintain biomechanical and hydrodynamic properties of the human valves.

With the long term aim of improving the clinical durability of cryopreserved allografts supplied to surgeons for use in patients in the UK, we have developed robust decellularisation processes for human donor aortic and pulmonary heart valves, based on the use of low concentration sodium dodecyl sulphate (SDS). A fully comprehensive description of the process and biological characteristics of the decellularised roots has been reported previously (Vafaee et al., 2016). The aim of this part of the study was to investigate the influence of decellularisation on the hydrodynamic performance and biomechanical properties of the low concentration SDS decellularised human aortic and pulmonary roots.

To the best of the authors' knowledge, this is the first full report comparing in vitro biomechanical and hydrodynamic properties of decellularised cryopreserved aortic and pulmonary human allografts with conventionally used cryopreserved aortic and pulmonary human

allografts.

2. Materials and methods

NHS Blood & Transplant Tissue & Eye Services (NHS BT TES), Speke, Liverpool, UK, supplied the human donor aortic and pulmonary roots used in this study. Ethical approval was obtained from the Yorkshire and the Humber committee – Leeds West, UK under the REC reference 09/H1307/82. Both the cellular and decellularised roots were cryopreserved using the standard NHS BT TES process and stored at −80 °C prior to use. The day before testing, the roots were thawed and stored at 4 °C in Cambridge antibiotic solution (Source BioScience; 80 rpm).

2.1. Study experimental design

This study was conducted in two phases (Fig. 1). In Phase I, the effect of decellularisation on the biomechanical and hydrodynamic properties of human aortic and pulmonary roots was investigated by comparison to cellular valve allografts (unpaired controls). The decellularised tissue was prepared as reported by Vafaee et al. which included the removal of excess fat and connective tissue, and scraping of the adventitial layer of the valve root using a scalpel blade (referred to throughout as 'scraping'), to allow diffusion of decellularisation solutions to achieve complete decellularisation (Vafaee et al., 2016). During this phase, there was a concern that the scraping process to disrupt the outer layer of the adventitia may have compromised the structure of the vessel. This layer has an important role in the structural support of the vessel wall in preventing overstretching (Lu et al., 2004; Laflamme et al., 2006). Damage to the adventitial layer may adversely affect the biomechanical properties of the vessel. Moreover, when removed from the heart the pulmonary root is hardly supported by the thin right ventricle myocardium, whereas the aortic root is supported by the bulging thick left ventricle myocardium. Therefore, a second phase (Phase II) was introduced following a review of the Phase I results, using only pulmonary roots. The cellular roots were biomechanically tested to determine baseline values for their mechanical properties. The roots were then decellularised by one of two protocols (with and without scraping) and the influence of the two decellularisation processing techniques on the mechanical properties of the tissue was determined. Phase II of the study also investigated whether the competency test procedure used in Phase I was sufficient to allow basic replication of the physiological model by preserving crucial boundary conditions. Consequently, an additional boundary condition was introduced, by addition of an annulus support in the valve competency test during Phase II of the study. A repeated measure design was adopted in Phase II, in which multiple tests were performed on the same root before and after decellularisation. Therefore, each valve root served as its own control increasing the statistical power of the study design.

2.1.1. Phase I

Eight aortic roots from six male and two female human donors with mean age of 57 years (range 27–75 years) and eight pulmonary roots from six male and two female human donors with mean age of 68 years (range 44–84 years) were used in Phase I of the study. Four aortic roots (mean diameter 21.3 ± 2.7 mm) and four pulmonary roots (mean diameter 24.3 ± 2.4 mm) were used as the cellular tissue controls. Four aortic (mean diameter 23.3 ± 2.7 mm) and four pulmonary roots (mean diameter 24.8 ± 3.0 mm) were decellularised as previously described by Vafaee et al. Vafaee et al. (2016). Each root underwent sequential in vitro hydrodynamic and biomechanical test protocols carried out over two consecutive days [Fig. 1(a)].

2.1.2. Phase II

To investigate the influence of the scraping step on the mechanical properties of the roots, first, functional mechanical tests were carried out on all the cellular roots, the samples were then divided into two groups with each group assigned one of two decellularisation processing protocols either with or without the scraping step [Fig. 1(b)]. The sequence of biomechanical tests was then repeated on the decellularised roots. Throughout the series of tests, the dimensions of each root were measured. For this study, only pulmonary roots were used. Samples were from four male and four female human donors with a mean age 58 years (range 18–68 years) with a mean valve diameter 22.5 ± 1.34 mm.

2.2. Test methods used in phase I

2.2.1. Hydrodynamic performance I: competency test under static back pressure

Competency tests were performed in order to assess valve closure under a physiological static pressure range. The valve competency was measured in terms of leakage flow rate for the valve under static back pressure. The leakage flow rate was obtained by placing the valve in closed position under a column of 0.9% (w/v) saline to apply back pressure, the leakage across the closed valve was measured over time and expressed as ml/s for each root. The maximum static back pressure for aortic and pulmonary roots was 120 and 60 mmHg respectively and the time taken for the pressure of the test fluid to drop to 80 mmHg (for aortic roots) and 20 mmHg (for pulmonary roots) was recorded. When the maximum static back pressure was applied, the diameter of the root was measured 4–5 mm above the sinotubular junction using a Vernier calliper. The root was classified as competent if the pressure head had not dropped to its respective lower pressure limit within a cut-off period of 20 min (or leakage rate ≤ 1.28 ml/s) for pulmonary and 30 min (or leakage rate ≤ 0.85 ml/s) for aortic roots.

2.2.2. Hydrodynamic performance II: pulsatile flow testing

All roots were function tested in an upgraded Leeds pulsatile flow simulator (Fisher et al., 1986; Jennings et al., 2001) to evaluate the hydrodynamic performance of the valve roots. A viscoelastic impedance adapter (VIA; Vivitro System Inc., Victoria BC, Canada) was used to deliver a more physiological ventricle pressure and flow waveform in the simulator. This system allowed for physiological pressure and flow waveforms as well as recording of high speed videos of leaflet motion. The system is described in detail by Jennings et al. (2001). At minimum VIA compliance, the simulator was adjusted for heart rates 60, 72 and 80 bpm with corresponding stroke volumes 60, 70 and 80 ml for optimum cardiac output. The systemic pressure was held between 120 and 80 mmHg for aortic roots and 45–15 mmHg for pulmonary roots. Each test was repeated with the VIA adjusted to its maximum compliance setting to produce relevant physiological pressure and flow characteristics (Jennings et al., 2001) and the test parameters adjusted accordingly. To characterise the performance of the roots, the leaflet dynamics, transvalvular pressure gradient (ΔP) during forward flow, the root mean square (RMS) forward flow (Q_{RMS}), and effective orifice area (EOA) were evaluated. The EOA was calculated using the formula $EOA = Q_{RMS}(ml/s)/51.6\sqrt{\Delta P}$ (mmHg) (Gabbay et al., 1978). All flow and pressure sensor positioning, data acquisition and analysis were in accordance with ISO 5840 and tests were performed using physiological 0.9% (w/v) saline. In total, 16 root specimens were tested. A mechanical control valve was also tested and compared with previous results to verify the performance of the pulsatile flow rig prior to testing of the roots.

The results are expressed as transvalvular pressure gradient versus RMS forward flow and EOA. The leaflet dynamics were assessed using an AOS Technologies S-PRI high speed camera recording at a rate of 500 frames per second during a complete cardiac cycle under pulsatile conditions, when the heart rate was 72 bpm. Regurgitant volumes could be obtained from pulsatile flow testing, however these were considered unreliable due to artefactual flow oscillations in the root during diastole

and so were not included in the results.

2.2.3. Biomechanical performance I: expansion characteristics (dilation testing)

The circumferential expansion of each root was determined in terms of percentage dilation using a dilation test procedure. This test procedure was adapted from previous studies (Jennings et al., 2002; Korossis et al., 2005). An internal static pressure was applied in increments of at least 5 mmHg from 0 to 35 mmHg to each pulmonary root and 0–120 mmHg to each aortic root, or until the root could no longer sustain the applied pressure. An image of each root at each pressure increment was captured using a Canon digital SLR 550 D camera and analysed using ImageJ (Schneider et al., 2012). At each pressure increment, the mean percentage change in external diameter of the valve root was calculated. The results are presented as percentage change in diameter of the root as a function of increasing pressure. During the test procedure, the height of test fluid at the start of testing was different for each root, which added extra static pressure in each pressure measurement. To calculate the actual applied pressure, the height of the column of fluid was measured, converted to a pressure (mmHg) and added to all the measured pressure values. This resulted in discrete final pressure values for all the valves. The mean percentage dilation is presented at 20 mmHg for pulmonary and 40 mmHg for aortic roots.

It was not possible to perform dilation tests on one decellularised aortic and one decellularised pulmonary root as they leaked faster than the pressure could be applied.

2.2.4. Biomechanical performance II: material properties (uniaxial tensile testing and suture pull-out testing)

Two different biomechanical assessment methods were performed to determine the effect of decellularisation treatment on the material properties of the root tissues, uniaxial tensile testing and suture pull-out testing.

For the uniaxial tensile tests, tissue specimens were prepared with 10 mm gauge length and 5 mm width from each root wall in the axial and circumferential directions, and from the valve leaflets in the circumferential direction. Due to size limitations, the radial specimens from valve leaflets were 3 mm in width with a 6 mm gauge length. Tensile tests were performed using an Instron 3365 materials testing machine (Instron, Bucks, UK) fitted with a 50 N load cell. A strain rate of 10 mm/min was used, similar to that previously reported in studies of human thoracic aorta (Duprey et al., 2010), mitral valve tissue (Kunzelman and Cochran, 1992) and porcine pulmonary valve tissue (Luo et al., 2014). The samples were hydrated using phosphate buffered saline solution (PBS; MP Biomedicals, LLC) maintained at 37 °C. The test specimens were gripped using bespoke light weight titanium grips, to eliminate tissue slippage or premature failure. Each tissue specimen thickness was measured with a digital thickness gauge J-40 V to a resolution of 0.01 mm.

The output load-extension curve was converted into a stress-strain curve from which the ultimate tensile stress (UTS), failure strain and slopes for the elastin and collagen phases were determined as previously described by Hasan et al. Hasan et al. (2014).

For suture pull out testing, the wall and myocardial specimens were cut from each root into rectangular specimens of 20 mm length and 15 mm width. At 4 mm from the short edge of the rectangular section, a 4-0 non-absorbable monofilament suture Premilene®, (Karck and Haverich, 2005; Park et al., 2012) was inserted and tied to form a loop. The sample was set up in an Instron 3365 materials testing machine (Instron, Bucks, UK) with a 50 N load cell. The tissue was clamped using one end of the previously described grips, the other end of the grips was used to clamp the looped suture. Using a strain rate of 10 mm/min, tension was applied to the suture until it was pulled out of the specimen. The peak load was recorded as the maximum suture pull-out force.

Due to the quality and variability between cellular human aortic valves, it was difficult to prepare adequate samples, especially from leaflets. Therefore, four additional cellular aortic valve roots were used for tensile and suture pull-out testing; a total of eight cellular aortic and four decellularised aortic roots. However, one decellularised and two cellular aortic circumferential leaflet specimens were excluded from the analysis because the initial linear region of the stress - strain curve to derive elastin phase modulus, was not distinct. Hence, six cellular and three decellularised samples were used for the mean elastin phase slope calculation.

2.3. Test methods used in phase II

In addition to the methods described in Phase I, to more fully assess the effect of the decellularisation processing method on the valve roots, it was considered necessary to carry out further functional biomechanical assessments and dimensional measurements.

2.3.1. Dimension measurement

To determine whether any physical dimensional changes of the pulmonary roots occurred after wall scraping or decellularisation treatment, the dimensions of each root were measured by taking an image of the root with a Canon digital SLR 550 D camera, which was then quantified with the imaging software (Image Pro Plus) with an accuracy of ± 5%. Each root was measured as a control and then re-measured after each process or treatment whilst maintaining the same conditions as the control. The change in size was calculated by comparing the specimen dimension after scraping and after the decellularisation treatment to the original dimension of the corresponding root.

2.3.2. Functional biomechanical assessment (competency under static back pressure and dilation)

Following dimension measurement, the competency of each root under static back pressure was determined adopting the same method used in Phase I (Section 2.2.1). A modification was made to the Phase I competency test method to set a more physiological boundary condition, by supporting the annulus of the valve with an annulus ring (Fig. 2). The expansion characteristics of the valve were determined in terms of percentage dilation for each root, using the same parameters as those applied in Phase I (Section 2.2.3). The mean percentage dilation was determined at 20 mmHg for all pulmonary roots.

It was not possible to perform a dilation test on one of the cellular pulmonary roots as it leaked faster than the pressure could be applied. Also, the age of one donor was an outlier hence dilation data for that valve was not included in the mean.

3. Statistics

For all the hydrodynamic performance and biomechanical characterisation tests used in Phase I, statistical significance between the cellular and decellularised aortic roots, and between the cellular and decellularised pulmonary roots, was determined using Student's *t*-test. In Phase II, statistical significance between all the pulmonary groups (cellular un-scraped, cellular scraped, decellularised un-scraped, decellularised scraped) was determined using one - way ANOVA. A significance level of $p < 0.05$ was applied. Statistical analyses were performed using SPSS for Windows (version 21.0; SPSS, Inc., USA).

The data associated with this paper are openly available from the University of Leeds Data Repository (Desai et al., 2017).

4. Results

4.1. Phase I

4.1.1. Effect of decellularisation on human pulmonary roots

The competency of decellularised pulmonary roots was determined

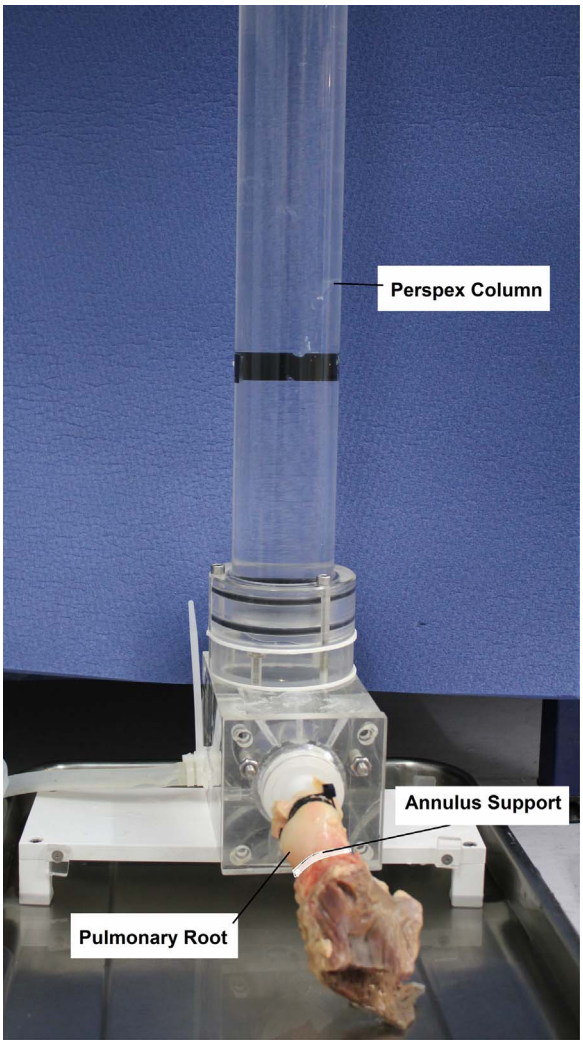

Fig. 2. Schematic of the root competency (with annulus support) test.

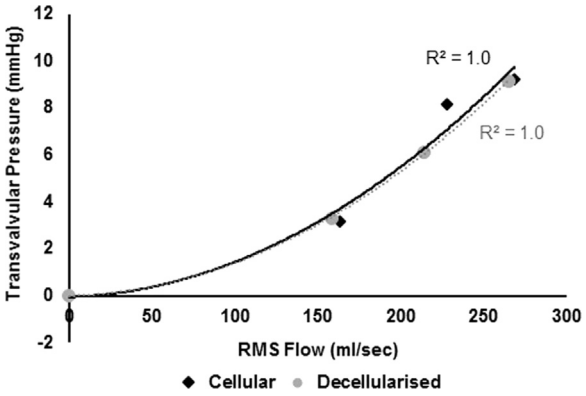

Fig. 3. Hydrodynamic assessment of human cellular and decellularised pulmonary roots. Mean transvalvular pressure gradient with respect to RMS flow for cellular (n = 4) and decellularised (n = 4) pulmonary roots – Data fitted with a second order polynomial trend line.

in terms of leakage rate and compared with the cellular roots. None of the four decellularised roots were considered fully competent as they had leakage rates higher than 1.28 ml/s. One valve root demonstrated severe regurgitation with a leakage rate of 17.25 ml/s whilst the mean leakage of the other three valve roots was 4.61 ml/s. In contrast, two of the four cellular pulmonary roots were classified as competent as they had a leakage rate less than the competency limit (≤ 1.28 ml/s); the other two roots were not competent and had a mean leakage rate of 3.68 ml/s. To better elucidate the circumferential expansion characteristics, and compare them with cellular, diameters of the cellular and decellularised pulmonary roots were measured at 60 mmHg pressure during the competency testing. At 60 mmHg static pressure, measured conduit diameters were in range of 28–37 mm for decellularised roots and 29.8–31 mm for cellular roots.

The mean transvalvular pressure gradient as a function of root mean square forward flow averaged for the decellularised and cellular pulmonary root is shown in Fig. 3. The decellularised pulmonary roots demonstrated similar hydrodynamic performance to cellular roots. The mean EOA for the decellularised pulmonary roots was also very similar to that of cellular roots (2.10 ± 0.36 cm^2 vs 2.31 ± 0.39 cm^2 respectively, p = 0.5).

Typical images of the decellularised and cellular pulmonary roots during a cardiac cycle with heart rate 72 bpm are shown in Fig. 4(a). Synchronous leaflet opening was observed for all the cellular pulmonary roots, producing a circular orifice. During diastole, the leaflets moved inwards, producing nearly perfect closing configuration with minor or no visible central leakage orifice for most of the cellular roots.

Synchronous and triangular leaflet opening, followed by circular orifice was observed for most of the decellularised pulmonary roots during systole. Two decellularised pulmonary roots showed incomplete leaflet coaptation where the leaflets edges appeared to be taut, resulting in large central and at commissural region regurgitant orifices Fig. 4(b). In contrast, the remaining two decellularised pulmonary roots appeared to be competent since only a minor central leakage orifice was observed Fig. 4(b). In addition, in some of the pulmonary valve leaflets (cellular and decellularised), pre-existing fenestrations were observed.

When dilated, the increase in external diameter of the decellularised pulmonary roots at an internal static pressure of 20 mmHg was significantly (p = 0.002) larger than the cellular roots with diameters of 12.9 ± 4.3% and 6.2 ± 2.0% respectively.

The tensile biomechanical properties of decellularised pulmonary roots compared to those of cellular roots are shown in Table 1. The decellularised wall showed no significant ($p > 0.05$) variation in the biomechanical tensile properties of interest, compared to the cellular tissue when tested either axially or circumferentially. However, the decellularised leaflets showed a higher UTS in the circumferential direction, and a lower UTS in the radial direction compared to cellular leaflets ($p < 0.05$). The mean collagen phase slope for decellularised leaflets in the circumferential direction was approximately double that of the cellular tissue (p = 0.008). Failure of both the wall and leaflet tissue occurred at or near to the centre of the gauge length.

The mean maximum force to pull a suture through wall and myocardial specimens for decellularised pulmonary roots was 3.18 ± 1.04 and 2.14 ± 0.56 N, respectively and not significantly different (ANOVA, $p > 0.05$) than cellular specimens (3.37 ± 2.84 N and 1.97 ± 1.02 N for wall and myocardium respectively). All the specimens failed by rupture of tissue in the circumferential direction perpendicular to the direction of the testing.

4.1.2. Effect of decellularisation on human aortic roots

All four decellularised aortic roots were not considered competent (having a leakage rate of > 0.85 ml/s); however the mean leakage rate for three of four decellularised aortic roots was below 10 ml/s. Three of four cellular aortic roots had a leakage rate less than or equal to 0.85 ml/s, with the remaining one having a leakage rate of 1.78 ml/s. At 120 mmHg static pressure, the diameters for decellularised roots were in the 28–42 mm range and; for cellular roots, the root diameters were between the 28–34 mm range. Moreover, for the decellularised aortic root with the poorest performance, the leakage rate was greater than 18 ml/s with a conduit diameter of 42 mm.

The transvalvular pressure gradients across the decellularised aortic roots were similar to the cellular roots (Fig. 5) and the mean EOA for

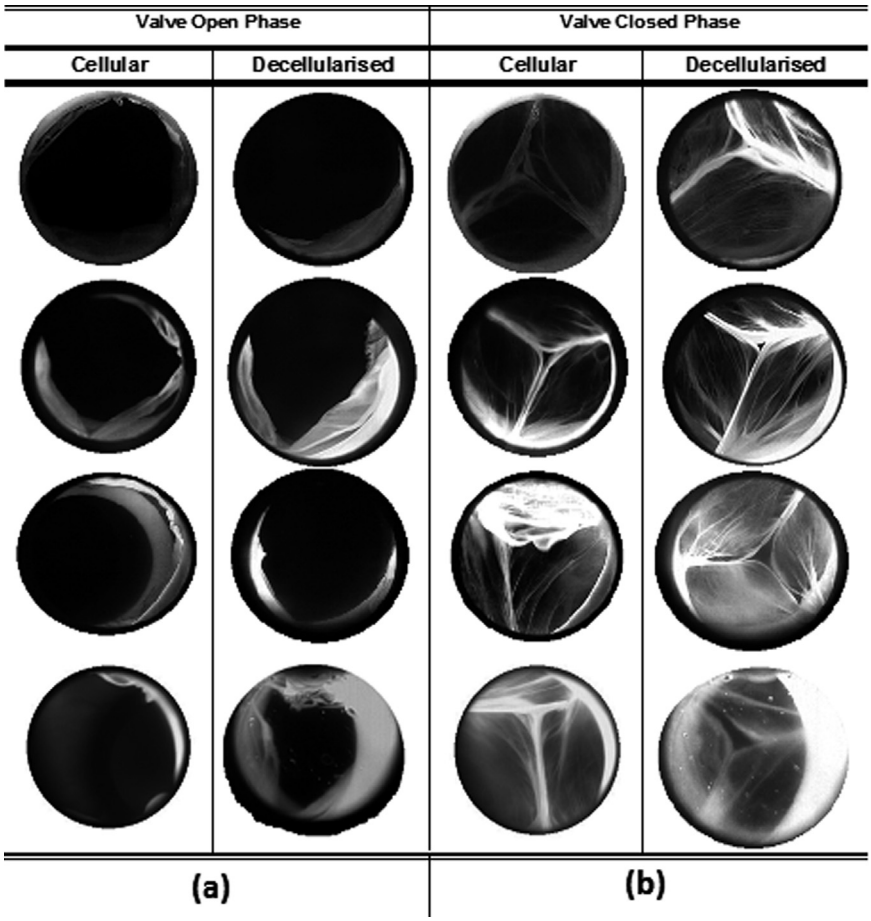

Fig. 4. Leaflet kinematics [(a) fully open (b) fully closed] of cellular and decellularised pulmonary roots at heart rate 72 bpm.

Table 1
Biomechanical parameters (collagen phase slope E_c, elastin phase slope E_e, ultimate tensile stress σ_{UTS}, failure strain $\varepsilon_{failure}$) based on the engineering stress versus engineering strain behaviour of cellular and decellularised pulmonary wall (axial (A) and circumferential (C) directions) and leaflet specimens (radial (R) and circumferential (C) directions).

Pulmonary Roots	E_c MPa	E_e MPa	σ_{UTS} MPa	$\varepsilon_{failure}$ %
Wall (A) Cellular	2.14 ± 0.70	0.15 ± 0.18	0.83 ± 0.28	85.62 ± 27.88
Decellularised	1.59 ± 0.55	0.10 ± 0.02	0.59 ± 0.20	84.04 ± 38.45
Wall (C) Cellular	3.20 ± 3.95	0.10 ± 0.02	1.35 ± 1.28	93.29 ± 23.29
Decellularised	4.23 ± 2.71	0.15 ± 0.14	1.42 ± 0.79	70.00 ± 29.79
Leaflet (R)	3.81 ± 3.73	0.33 ± 0.75	0.53 ± 0.30	33.19 ± 13.78
Cellular	1.76 ± 1.33	0.33 ± 0.43	0.20 ± 0.13*	24.01 ± 18.42
Decellularised				
Leaflet (C)	15.44 ± 9.72	1.07 ± 1.72	1.54 ± 0.84	17.12 ± 5.36
Cellular	29.50 ± 6.31*	1.80 ± 2.18	3.28 ± 0.73*	17.83 ± 5.76
Decellularised				

Data are expressed as the mean (n = 4) ± 95% confidence limits.
* -Statistically significance difference ($p < 0.05$) for decellularised versus cellular pulmonary roots.

the decellularised roots was not significantly different from cellular roots (1.55 ± 0.54 cm^2 and 1.29 ± 0.39 cm^2 for decellularised and cellular roots respectively; p = 0.26).

Images from the high - speed video recording of leaflet kinematics for the cellular and decellularised aortic roots are shown in Fig. 6. During the opening phase, two of the four cellular aortic roots had a triangular orifice, which then changed to a circular orifice when the valve reached its fully open position. However, for two of the cellular aortic roots, partial leaflet opening was observed. The fully closed leaflet configuration was excellent for two of the cellular aortic roots with no visible central leakage orifice and a minor central leakage orifice was observed in the two remaining cellular roots.

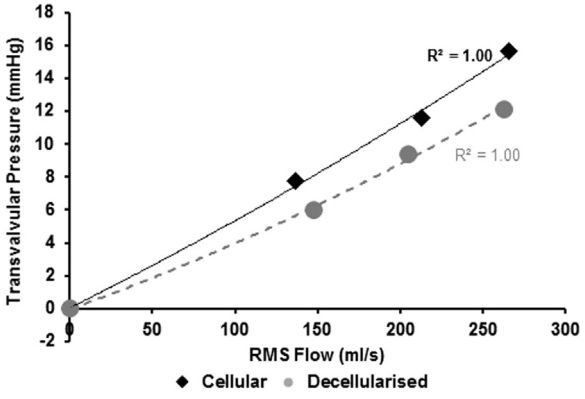

Fig. 5. Hydrodynamic assessment of cellular and decellularised aortic roots. Mean transvalvular pressure gradient with respect to RMS flow for cellular (n = 4) and decellularised (n = 4) aortic roots – Data fitted with a second order polynomial trend line.

For most of the decellularised aortic roots, the leaflets opened fully or near-fully, producing circular or near-circular orifices. However, for one of the decellularised aortic roots, the leaflets did not fully open resulting in a restricted triangular orifice. All the decellularised aortic roots appeared competent since a central leakage orifice was negligible or not observed during closed phase.

The expansion characteristics of decellularised aortic roots were similar to cellular roots at an internal pressure of 40 mmHg. The

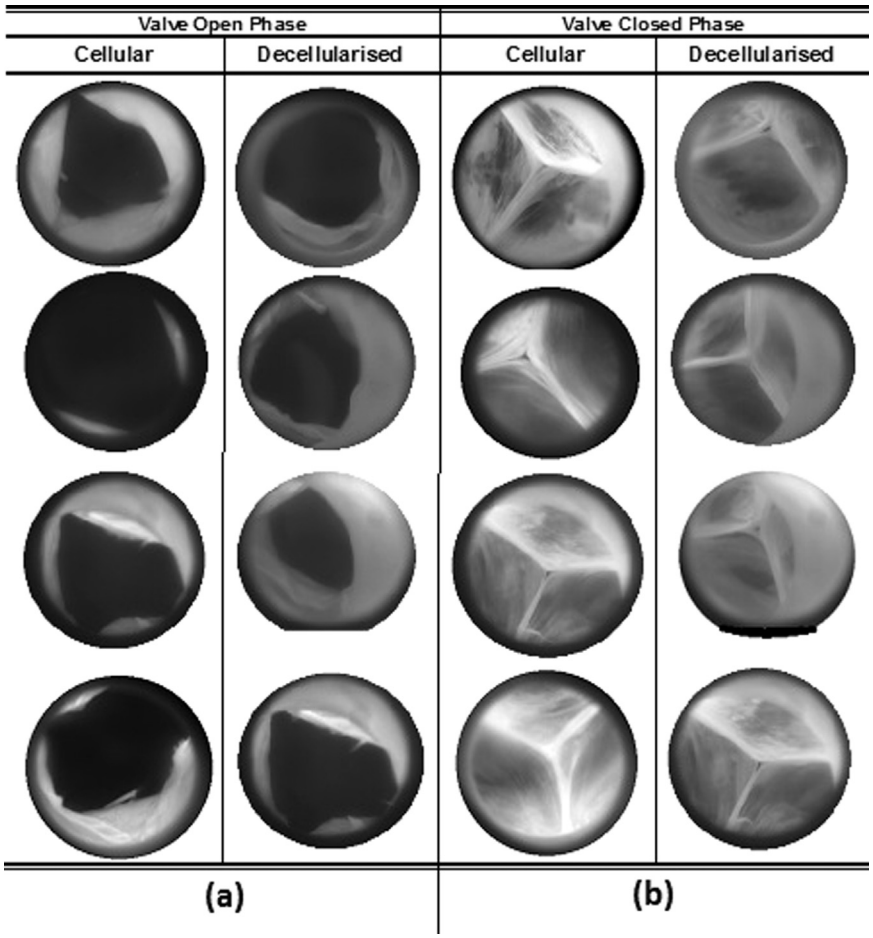

Fig. 6. Leaflet kinematics [(a) fully open (b) fully closed] of cellular and decellularised aortic roots at heart rate 72 bpm.

external wall diameters of the decellularised and cellular aortic roots dilated by 12.6 ± 2.6% and 15.4 ± 5.4% respectively, which were not significantly different ($p = 0.23$).

The biomechanical parameters, obtained from uniaxial tensile testing of wall and leaflets for the decellularised and cellular aortic roots, are listed in Table 2. A comparison between the decellularised and cellular aortic roots revealed no significant difference between the wall parameters in both the axial and circumferential directions ($p > 0.05$). A significant increase in the elastin phase modulus in the circumferential direction and collagen phase in the radial direction was observed in the decellularised aortic leaflet specimens in comparison to the cellular leaflet specimens ($p < 0.001$). In addition, decellularised aortic leaflet specimens demonstrated greater UTS in the radial and circumferential directions than cellular leaflet specimens ($p < 0.05$).

Following suture pull-out testing of the cellular and decellularised aortic specimens, the wall and myocardial decellularised specimens had suture retention strength values of 6.63 ± 1.90 N and 6.12 ± 7.83 N respectively, which were not significantly different from the corresponding cellular wall and myocardial values of 6.87 ± 3.26 N and 5.71 ± 1.07 N respectively ($p > 0.05$).

Table 2
Biomechanical parameters (collagen phase slope E_c, elastin phase slope E_e, ultimate tensile stress σ_{UTS}, failure strain $\varepsilon_{failure}$) based on the engineering stress versus engineering strain behaviour of cellular and decellularised aortic wall (axial (A) and circumferential (C) directions) and leaflet specimens (radial (R) and circumferential (C) directions).

Aortic Roots	E_c MPa	E_e MPa	σ_{UTS} MPa	$\varepsilon_{failure}$ %
Wall (A) Cellular	1.72 ± 1.09	0.14 ± 0.10	0.72 ± 0.27	86.04 ± 15.26
Decellularised	1.98 ± 1.07	0.16 ± 0.17	0.82 ± 0.44	78.29 ± 45.09
Wall (C) Cellular	3.23 ± 0.74	0.19 ± 0.07	1.47 ± 0.68	89.14 ± 36.95
Decellularised	4.24 ± 2.64	0.21 ± 0.09	1.44 ± 0.42	73.50 ± 51.90
Leaflet (R)	1.30 ± 0.56	0.04 ± 0.04	0.19 ± 0.07	32.29 ± 8.18
Cellular	4.06 ± 2.56*	0.15 ± 0.18	0.59 ± 0.21*	29.86 ± 10.37
Decellularised				
Leaflet (C)	11.91 ± 7.18	0.36 ± 0.25	1.40 ± 0.56	21.29 ± 6.86
Cellular	20.62 ± 9.08	1.76 ± 0.92*	2.41 ± 1.02*	16.41 ± 2.22
Decellularised				

Data are expressed as the mean ± 95% confidence limits. n = 8 for cellular and n = 4 for decellularised for all data, except for elastin phase in the circumferential direction where n = 6 for cellular and n = 3 for decellularised.

* -Statically significant difference ($p < 0.05$) for decellularised versus cellular roots.

4.2. Phase II

4.2.1. Effect of decellularisation treatment and processing (scraping) on geometry of human pulmonary roots

The dimensions of the pulmonary roots were measured before and after scraping, and after the decellularisation treatment. The changes in dimensions were calculated and compared. There was no clear effect of the scraping procedure or decellularisation treatment on the dimensions of the pulmonary roots.

4.2.2. Effect of decellularisation treatment and processing (scraping) on the valve competency and dilation properties of the human pulmonary roots

To access the competency with a more appropriate physiological boundary condition, each pulmonary root (n = 8) was tested without and with an annulus support ring under static back pressure. Seven of

the eight cellular pulmonary roots had leakage rates greater than 1.28 ml/s without annulus support. After scraping and decellularisation treatment, all the pulmonary roots had a leakage rate greater than 1.28 ml/s without annulus support. With annulus support however, five out of eight cellular un-scraped and all four cellular scraped pulmonary roots were competent, with leakage rate under 1.28 ml/s. After decellularisation treatment the mean static leakage rate for these un-scraped and scraped pulmonary roots was under 2.5 ml/s when tested with annulus support with the exception of one conduit (4.4 ml/s). Experimental difficulties were experienced with one root when tested before decellularisation without annulus ring, as it leaked faster than the static pressure applied and it had the highest mean flow rate of 26.0 ml/s when the annulus was supported. However, after decellularisation, the valve root appeared competent with its leakage flow rate reduced to 1.01 ml/s. These results showed that the annulus ring helped to restore the shape and size of the valve annulus to its physiological geometry.

In order to assess the effects of scraping and decellularisation on the expansion characteristics of pulmonary roots, the percentage dilation was measured for cellular un-scraped, cellular scraped, decellularised un-scraped and decellularised scraped roots. The percentage dilation was recorded at 20 mmHg pressure for all the types of valves studied and the mean values were determined Fig. 7. The dilation characteristics of these pulmonary roots showed no significant variation.

5. Discussion

It was hypothesised that after decellularisation, hydrodynamic and biomechanical properties of the human pulmonary and aortic roots would be minimally affected or maintained when compared with their cellular counterparts due to the preservation of the extracellular matrix (ECM). During the decellularisation treatment, complete cell removal was demonstrated histologically and biochemically (Vafaee et al., 2016) however, it is crucial to retain the tissue function and biomechanical properties whilst completely removing all cellular components.

5.1. Effect of decellularisation on hydrodynamic and biomechanical properties of the human pulmonary roots

Clinically, it is important for any replacement heart valves to have low transvalvular pressure gradients, with minimum leakage through the closed valve and leaflets that co-apt to function properly as in the native cellular valve. For the decellularised pulmonary roots, good hydrodynamic function was observed with low transvalvular pressure gradients and EOAs comparable to cellular roots. Additionally, the leaflet kinematics observed for most of the decellularised pulmonary roots were similar to those of the cellular roots, which has implications for long-term durability.

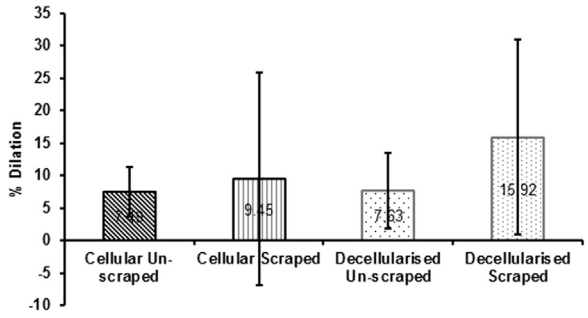

Fig. 7. Mean percentage dilation at 20 mmHg for the pulmonary cellular un-scraped roots (n = 6), cellular scraped roots (n = 3), decellularised un-scraped roots (n = 3), decellularised scraped roots (n = 3). Data is presented as the mean ± 95% confidence limits. Data was analysed by one-way analysis of variance which revealed no significant variation in the data.

Maintaining competency of tissue heart valves is dependent on the coordinated actions of the annulus, leaflets and associated wall collectively. Therefore, stiffening or dilation of the wall or stiffening of leaflets can hinder proper coaptation of the valve leaflets during closure and thereby promote regurgitation (Sabbah et al., 1986). Competency testing was performed to assess the valve closure under a static back pressure. In Phase I, the competency test results for the pulmonary roots showed uncertainty with respect to reliability of the test method as most of the valves had a leakage rate > 1.28 ml/s. In the test method used, a spigot supported the wall of the root however, the thin, delicate myocardium of pulmonary roots was not supported. It was decided that the test conditions used did not provide realistic anatomical conditions, which may have contributed to the high closed valve regurgitation rate and it became apparent that a new or modified in vitro model was needed for valve competency testing. For this reason, in Phase II, the setup for valve competency testing was modified to incorporate an annulus ring in order to mimic the support provided from the heart. The new test methodology was particularly useful in testing of the pulmonary roots. Under the modified test conditions, the results showed that the majority of the decellularised pulmonary roots exceeded the set competency limit, allowing minimum back flow under physiological static back pressure.

The expansion characteristics of the pulmonary wall with respect to internal pressure is important for the geometry and function of implanted allograft valves (Lockie et al., 1993). Following decellularisation, it is important to monitor the expansion characteristics of roots as over- expansion of the root may have damaging effects on closed valve stresses (Christie and Barratt-Boyes, 1995). In Phase I, full understanding of the expansion characteristics of decellularised pulmonary roots could not be obtained due to lack of pre-decellularisation processing data. It was hypothesised that the scraping process may have induced disruption in the wall mechanical properties, as studies have shown that the adventitia layer provides structural support and protects vessels from overstretch (Lu et al., 2004; Laflamme et al., 2006). Therefore Phase II of the study was introduced to investigate the influence of the scraping step in the decellularisation protocol on the biomechanical properties of the roots. The Phase II study made a paired comparison and showed that the scraping of the adventitia of the wall or decellularisation treatment had no significant effect on the expansion properties of the pulmonary roots. Although, high 95% confidence limits were observed in the dilation test results (Phase II), particularly within the scraped cellular and scraped decellularised pulmonary roots. These large confidence limits may be attributed to the small number of samples used in the calculation of the mean value.

The biomechanical tensile and suture pull out tests for the pulmonary roots showed no significant differences between cellular and decellularised wall parameters. This leads to the conclusion that the root wall maintains its natural mechanical tensile properties following decellularisation possibly due to the preservation of the elastin and collagen content of the tissue. For the leaflets however, this was not the case. The decellularised pulmonary leaflets were significantly stiffer in the collagen dominant phase and failed at significantly higher UTS than the cellular leaflets in the circumferential direction. Such changes may be due to the significant reduction of glycosaminoglycan (GAGs) and removal of cells reported by Vafaee et al. (2016). The loss of GAGs in the decellularised leaflets, may have led to loosening of the fibrous structure, and uncrimping of the circumferentially aligned collagen fibers. This could potentially cause an earlier than normal recruitment and reorientation of the collagen fibers in the direction of applied strain during tensile testing (Williams et al., 2009). Previous work on decellularised tissues has shown similar findings in bone tissue (Banse et al., 2002), ligaments (Frank et al., 1995; Herbert et al., 2016) and soft tissue (Freed and Doehring, 2005). It is expected that the leaflets of the decellularised roots will recellularise in vivo and regain their physiological tensile properties. The extensibility of decellularised pulmonary

leaflets was comparable to the cellular leaflets in both the radial and circumferential directions, while UTS for decellularised specimens was significantly reduced in the radial direction. Previous results on porcine pulmonary roots decellularised with a similar protocol did not show leaflet stiffening but showed wall stiffening in both the axial and circumferential directions in the initial elastin phase (Luo et al., 2014). Nevertheless, these findings related to material properties of the decellularised pulmonary roots showed that the resultant changes due to decellularisation treatment can be highly dependent on species, tissue type and method (Gilbert et al., 2006), which highlights the need to carry out robust pre-clinical testing of all types of decellularised tissues prior to their implantation.

Several studies have reported short-term and medium-term in vivo performance of the CryoValve SynerGraft (CryoLife Inc, Kennesaw, GA) decellularised pulmonary human heart valves in comparison to standard cryopreserved allografts (Bechtel et al., 2008; Konuma et al., 2009; Burch et al., 2010; Brown et al., 2011). Overall, 399 CryoValve SynerGraft pulmonary human heart valves were implanted in several centers for pulmonary valve replacement between 2000 and 2005 and results were favourable with respect to structural deterioration and endocarditis. da Costa et al. have demonstrated that decellularised pulmonary allografts showed excellent hemodynamic behaviour and reduction in immunogenic response compared to standard allografts in RVOT (da Costa et al., 2005). Another recent study by da Costa reported higher reoperation-free survival with decellularised pulmonary allografts compared to conventional cryopreserved allografts for RVOT reconstruction up to 6 years of follow-up, and, in addition, pressure gradients were lower in the decellularised pulmonary allografts (da Costa et al., 2014).

5.2. Effect of decellularisation on hydrodynamic and biomechanical properties of the aortic roots

The in vitro hydrodynamic comparison of decellularised aortic roots with cellular roots showed lower mean transvalvular pressure gradients for all the tested conditions, indicating a reduced resistance against forward flow.

The wall tensile parameters of the decellularised aortic roots were similar to those of the cellular aortic roots. However, the decellularised leaflets became stiffer and significantly stronger than cellular leaflets in the circumferential direction which could be due to loosening and uncrimping of the collagen fiber network (Freed and Doehring, 2005) leading to increased stiffness of the tissue. Also, results from this study showed that the extensibility of the decellularised circumferential aortic leaflet specimens was higher than the cellular specimens. Furthermore, decellularised leaflet specimens were significantly stiffer and stronger in the radial direction. The findings from this study correlated well with a previous study which tested porcine aortic leaflets and found that after decellularisation treatment, their extensibility and failure strain significantly increased in the circumferential direction, while in the radial direction, the increase in strength was not significant (Korossis et al., 2002). Nonetheless, consideration must be taken to allow for species-related differences when interpreting these results. Although, the strength and stiffness of the aortic leaflets was affected by the decellularisation procedure, it did not appear to negatively affect valve function. Moreover, the expansion characteristics of the decellularised aortic wall were similar to cellular aortic wall in the physiological pressure range, contributing to its positive performance.

Decellularised aortic allograft valves are already delivering promising in vivo results. Zehr and colleagues reported favourable clinical results on the use of Synergraft decellularised aortic valve allografts for aortic valve replacement (Zehr et al., 2005). The valves have been implanted in patients with a mean age of 53 ± 14 years. Although the small number of patients and short term mean follow up (30.3 months) limits the results, Zehr et al. demonstrated no calcification in wall or leaflets with stable hemodynamic function without major complications during echocardiography. Calcification rarely occurs immediately after implantation, hence long term results are required. da Costa et al. implanted decellularised aortic allografts in 41 patients with a mean age of 34 years. The post-operative results showed stable structural integrity, low rate of calcification, and adequate hemodynamics in the short term follow–up (maximum 19 months); however, one patient underwent reoperation due to mitral valve stenosis (da Costa et al., 2010). Tudorache et al. analysed results of 69 decellularised aortic allograft implants in children and young patients. Hemodynamic performance of these decellularised allografts was excellent up to 7.6 years of follow up. Most importantly, this study showed clinical data of decellularised aortic allograft implanted in 16 patients younger than 10 years (Tudorache et al., 2016). The data from this younger group of patients raised concerns about supravalvular stenosis and valvular regurgitation. However, the mean short term follow up, small number of patients and complex surgical procedure in these young patients, limit the discussion of the results. Overall the results from these studies (da Costa et al., 2010; Zehr et al., 2005; Tudorache et al., 2016) are promising; even though the decellularisation protocols were slightly different to the decellularisation protocol used in this study, this can nevertheless be seen as another sign of the excellent preliminary results achieved using decellularised allografts.

6. Limitations

There are several limitations to this study. First, the in vitro nature of this study meant the test methodologies used were a simplification of the environmental conditions under which the decellularised roots will be placed in vivo; there was also no consideration of the effects of inflammation, cell repopulation or tissue remodelling, all of which may influence the mechanical properties and flow characteristics of the valves. Second, the relatively small sample size meant a lack of statistical power to discriminate/provide significant differences between biomechanical properties of the cellular and decellularised roots. The statistical power was also influenced by inherent biological variation and quality of the tissue.

7. Conclusion

In conclusion, an extensive in vitro hydrodynamic and biomechanical comparison of decellularised and cellular human aortic and pulmonary roots has been performed. Neither hydrodynamic nor expansion properties of human pulmonary and aortic roots were significantly affected by the low concentration SDS decellularisation treatment. Decellularisation, however, significantly altered some of the directional material properties of pulmonary and aortic valve leaflets. Despite these changes in leaflet material properties, the magnitude of these changes may not be large enough to influence the performance of the valves in vivo, as these decellularised human heart valves showed excellent hydrodynamic properties, compared to cellular counterparts. Findings from this study will serve as a step forward to using the low concentration SDS decellularised human allografts for clinical trials.

Acknowledgments

We would like to thank the donors and their families.

This work was supported by the Innovation and Knowledge Centre in Medical Technologies funded by the EPSRC, TSB and BBSRC. It was partially funded through WELMEC, a Centre of Excellence in Medical Engineering funded by the Wellcome Trust and EPSRC under grant number WT 088908/Z/09/Z.

Disclosure statement

E. Ingham, J. Fisher and HE Berry are shareholders in and consultants to Tissue Regenix Group PLC.

References

Alpert, J.S., Dalen, J.E., 1987. Changing concepts in the diagnosis and management of patients with valvular heart-disease – a clinicians view. Z. Kardiol. 76, 81–84.

Alsoufi, B., Al-Halees, Z., Manlhiot, C., McCrindle, B.W., Al-Ahmadi, M., Sallehuddin, A., Canver, C.C., Bulbul, Z., Joufan, M., Fadel, B., 2009. Mechanical valves versus the Ross procedure for aortic valve replacement in children: propensity-adjusted comparison of long-term outcomes. J. Thorac. Cardiovasc. Surg. 137, 362–370. http://dx.doi.org/10.1016/j.jtcvs.2008.10.010.

Anssari-Benam, A., Bader, D.L., Screen, H.R.C., 2011. A combined experimental and modelling approach to aortic valve viscoelasticity in tensile deformation. J. Mater. Sci.-Mater. Med. 22, 253–262. http://dx.doi.org/10.1007/s10856-010-4210-6.

Banse, X., Sims, T.J., Bailey, A.J., 2002. Mechanical properties of adult vertebral cancellous bone: correlation with collagen intermolecular cross-links. J. Bone Miner. Res. 17, 1621–1628. http://dx.doi.org/10.1359/jbmr.2002.17.9.1621.

Bechtel, J.F., Stierle, U., Sievers, H.H., 2008. Fifty-two months' mean follow up of decellularized SynerGraft-treated pulmonary valve allografts. J. Heart Valve Dis. 17, 98–104 (discussion).

Billiar, K.L., Sacks, M.S., 2000. Biaxial mechanical properties of the native and glutaraldehyde-treated aortic valve cusp: part II - A structural constitutive model. J. Biomech. Eng.-Tran. ASME 122, 327–335. http://dx.doi.org/10.1115/1.1287158.

Booth, C., Korossis, S.A., Wilcox, H.E., Watterson, K.G., Kearney, J.N., Fisher, J., Ingham, E., 2002. Tissue engineering of cardiac valve prostheses I: development and histological characterization of an acellular porcine scaffold. J. Heart Valve Dis. 11, 457–462.

Brown, J.W., Ruzmetov, M., Eltayeb, O., Rodefeld, M.D., Turrentine, M.W., 2011. Performance of synergraft decellularized pulmonary homograft in patients undergoing a Ross procedure. Ann. Thorac. Surg. 91, 416–422. http://dx.doi.org/10.1016/j.athoracsur.2010.10.069.

Burch, P.T., Kaza, A.K., Lambert, L.M., Holubkov, R., Shaddy, R.E., Hawkins, J.A., 2010. Clinical performance of decellularized cryopreserved valved allografts compared with standard allografts in the right ventricular outflow tract. Ann. Thorac. Surg. 90, 1301–1305. http://dx.doi.org/10.1016/j.athoracsur.2010.05.024.

Cebotari, S., Lichtenberg, A., Tudorache, I., Hilfiker, A., Mertsching, H., Leyh, R., Breymann, T., Kallenbach, K., Maniuc, L., Batrinac, A., Repin, O., Maliga, O., Ciubotaru, A., Haverich, A., 2006. Clinical application of tissue engineered human heart valves using autologous progenitor cells. Circulation 114, I132–I137. http://dx.doi.org/10.1161/circulationaha.105.001065.

Christie, G.W., Barratt-Boyes, B.G., 1995. Age-dependent changes in the radial stretch of human aortic valve leaflets determined by biaxial testing. Ann. Thorac. Surg. 60, 156–159.

Courtman, D.W., Pereira, C.A., Kashef, V., McComb, D., Lee, J.M., Wilson, G.J., 1994. Development of a pericardial acellular matrix biomaterial: biochemical and mechanical effects of cell extraction. J. Biomed. Mater. Res. 28, 655–666. http://dx.doi.org/10.1002/jbm.820280602.

Cox, M.A.J., Driessen, N.J.B., Bouten, C.V.C., Baaljens, F.P.T., 2006. Mechanical characterization of anisotropic planar biological soft tissues using large indentation: a computational feasibility study. J. Biomech. Eng.-Trans. ASME 128, 428–436. http://dx.doi.org/10.1115/1.2187040.

da Costa, F.D.A., Dohmen, P.M., Duarte, D., von Glenn, C., Lopes, S.V., Haggi, H., da Costa, M.B.A., Konertz, W., 2005. Immunological and echocardiographic evaluation of decellularized versus cryopreserved allografts. during the Ross operation. Eur. J. Cardio-Thorac. Surg. 27, 572–577. http://dx.doi.org/10.1016/j.ejcts.2004.12.057.

da Costa, F.D.A., Costa, A., Prestes, R., Domanski, A.C., Balbi, E.M., Ferreira, A.D.A., Lopes, S.V., 2010. The early and midterm function of decellularized aortic valve allografts. Ann. Thorac. Surg. 90, 1854–1861. http://dx.doi.org/10.1016/j.athoracsur.2010.08.022.

da Costa, F.D.A., Takkenberg, J.J.M., Fornazari, D., Balbi, E.M., Colatusso, C., Mokhles, M.M., da Costa, A., Sagrado, A.G., Ferreira, A.D.D., Fernandes, T., Lopes, S.V., 2014. Long-term results of the Ross operation: an 18-year single institutional experience. European J. Cardio-Thorac. Surg. 46, 415–422. http://dx.doi.org/10.1093/ejcts/ezu013.

Desai, A., Vafaee, T., Rooney, P., Kearney, J.N., Berry, H.E., Ingham, E., Fisher, J., Jennings, L.M., 2017. In vitro biomechanical and hydrodynamic characterisation of decellularised human pulmonary and aortic roots- data set (https://doi.org/). Univ. Leeds Repos. http://dx.doi.org/10.5518/178.

Dignan, R., O'Brien, M., Hogan, P., Thornton, A., Fowler, K., Byrne, D., Stephens, F., Harrocks, S., 2003. Aortic valve allograft structural deterioration is associated with a subset of antibodies to human leukocyte antigens. J. Heart Valve Dis. 12, 382–391.

Dohmen, P.M., 2012. Clinical results of implanted tissue engineered heart valves. HSR Proc. Intens. Care Cardiovasc. Anesth. 4, 225–231.

Duprey, A., Khanafer, K., Schlicht, M., Avril, S., Williams, D., Berguer, R., 2010. In vitro characterisation of physiological and maximum elastic modulus of ascending thoracic aortic aneurysms using uniaxial tensile testing. Eur. J. Vasc. Endovasc. Surg. 39, 700–707. http://dx.doi.org/10.1016/j.ejvs.2010.02.015.

Edwards, M.B., Draper, E.R.C., Hand, J.W., Taylor, K.M., Young, I.R., 2005. Mechanical testing of human cardiac tissue: some implications for MRI safety. J. Cardiovasc. Magn. Reson. 7, 835–840. http://dx.doi.org/10.1080/10976640500288149.

Elkins, R.C., Dawson, P.E., Goldstein, S., Walsh, S.P., Black, K.S., 2001. Decellularized human valve allografts. Ann. Thorac. Surg. 71, S428–S432. http://dx.doi.org/10.1016/s0003-4975(01)02503-6.

Engelmayr, G.C., Rabkin, E., Sutherland, F.W.H., Schoen, F.J., Mayer, J.E., Sacks, M.S., 2005. The independent role of cyclic flexure in the early in vitro development of an engineered heart valve tissue. Biomaterials 26, 175–187. http://dx.doi.org/10.1016/j.biomaterials.2004.02.035.

Fisher, J., Jack, G.R., Wheatley, D.J., 1986. Design of a function-test apparatusapparatus for prosthetic heart-valves - initial results in the mitral position. Clin. Phys. Physiol. Measur. 7, 63–73. http://dx.doi.org/10.1088/0143-0815/7/1/005.

Frank, C., McDonald, D., Wilson, J., Eyre, D., Shrive, N., 1995. Rabbit medial collateral ligament scar weakness is associated with decreased collagen pyridinoline cross-link density. J. Orthop. Res. 13, 157–165. http://dx.doi.org/10.1002/jor.1100130203.

Freed, A.D., Doehring, T.C., 2005. Elastic model for crimped collagen fibrils. J. Biomech. Eng.-Trans. ASME 127, 587–593. http://dx.doi.org/10.1115/1.1934145.

Gabbay, S., McQueen, D.M., Yellin, E.L., Becker, R.M., Frater, R.W., 1978. In vitro hydrodynamic comparison of mitral valve prostheses at high flow rates. J. Thorac. Cardiovasc. Surg. 76, 771–787.

Gilbert, T.W., Sellaro, T.L., Badylak, S.F., 2006. Decellularization of tissues and organs. Biomaterials 27, 3675–3683. http://dx.doi.org/10.1016/j.biomaterials.2006.02.014.

Hasan, A., Ragaert, K., Swieszkowski, W., Selimovic, S., Paul, A., Camci-Unal, G., Mofrad, M.R.K., Khademhosseini, A., 2014. Biomechanical properties of native and tissue engineered heart valve constructs. J. Biomech 47, 1949–1963. http://dx.doi.org/10.1016/j.jbiomech.2013.09.023.

Hawkins, J.A., Breinholt, J.P., Lambert, L.M., Fuller, T.C., Profaizer, T., McGough, E.C., Shaddy, R.E., 2000. Class I and class II anti-HLA antibodies after implantation of cryopreserved allograft material in pediatric patients. J. Thorac. Cardiovasc. Surg. 119, 324–328. http://dx.doi.org/10.1016/s0022-5223(00)70188-7.

Herbert, A., Brown, C., Rooney, P., Kearney, J., Ingham, E., Fisher, J., 2016. Bi-linear mechanical property determination of acellular human patellar tendon grafts for use in anterior cruciate ligament replacement. J. Biomech. 49, 1607–1612. http://dx.doi.org/10.1016/j.jbiomech.2016.03.041.

Jennings, L.M., Butterfield, M., Walker, P.G., Watterson, K.G., Fisher, J., 2001. The influence of ventricular input impedance on the hydrodynamic performance of bioprosthetic aortic roots in vitro. J. Heart Valve Dis. 10, 269–275.

Jennings, L.M., Butterfield, M., Booth, C., Watterson, K.G., Fisher, J., 2002. The pulmonary bioprosthetic heart valve: its unsuitability for use as an aortic valve replacement. J. Heart Valve Dis. 11, 668–678.

Jordan, J.E., Williams, J.K., Lee, S.J., Raghavan, D., Atala, A., Yoo, J.J., 2012. Bioengineered self-seeding heart valves. J. Thorac. Cardiovasc. Surg. 143, 201–208. http://dx.doi.org/10.1016/j.jtcvs.2011.10.005.

Karck, M., Haverich, A., 2005. Aortic valve reimplantation according to the David type I technique. Oper. Tech. Thorac. Cardiovasc. Surg. 10, 246–258. http://dx.doi.org/10.1053/j.optechstcvs.2005.08.004.

Kidane, A.G., Burriesci, G., Cornejo, P., Dooley, A., Sarkar, S., Bonhoeffer, P., Edirisinghe, M., Seifalian, A.M., 2009. Current developments and future prospects for heart valve replacement therapy. J. Biomed. Mater. Res. Part B-Appl. Biomater. 88B, 290–303. http://dx.doi.org/10.1002/jbm.b.31151.

Konuma, T., Devaney, E.J., Bove, E.L., Gelehrter, S., Hirsch, J.C., Tavakkol, Z., Ohye, R.G., 2009. Performance of cryovalve SG decellularized pulmonarypulmonary allografts compared with standard cryopreserved allografts. Ann. Thorac. Surg. 88, 849–855. http://dx.doi.org/10.1016/j.athoracsur.2009.06.003.

Korossis, S.A., Booth, C., Wilcox, H.E., Watterson, K.G., Kearney, J.N., Fisher, J., Ingham, E., 2002. Tissue engineering of cardiac valve prostheses II: biomechanical characterization of decellularized porcine aortic heart valves. J. Heart Valve Dis. 11, 463–471.

Korossis, S.A., Wilcox, H.E., Watterson, K.G., Kearney, J.N., Ingham, E., Fisher, J., 2005. In-vitro assessment of the functional performance of the decellularized intact porcine aortic root. J. Heart Valve Dis. 14, 408–421.

Kunzelman, K.S., Cochran, R.P., 1992. Stress/strain characteristics of porcine mitral valve tissue: parallel versus perpendicular collagen orientation. J. Card. Surg. 7, 71–78.

Laflamme, K., Roberge, C.J., Grenier, G., Remy-Zolghadri, M., Pouliot, S., Baker, K., Labbe, R., D'Orleans-Juste, P., Auger, F.A., Germain, L., 2006. Adventitia contribution in vascular tone: insights from adventitia-derived cells in a tissue-engineered human blood vessel. FASEB J. 20, 1245–1247. http://dx.doi.org/10.1096/fj.05-4702fje.

Liao, J., Joyce, E.M., Sacks, M.S., 2008. Effects of decellularization on the mechanical and structural properties of the porcine aortic valve leaflet. Biomaterials 29, 1065–1074. http://dx.doi.org/10.1016/j.biomaterials.2007.11.007.

Lichtenberg, A., Tudorache, I., Cebotari, S., Ringes-Lichtenberg, S., Sturz, G., Hoeffler, K., Hurscheler, C., Brandes, G., Hilfiker, A., Haverich, A., 2006. In vitro re-endothelialization of detergent decellularized heart valves under simulated physiological dynamic conditions. Biomaterials 27, 4221–4229. http://dx.doi.org/10.1016/j.biomaterials.2006.03.047.

Lockie, K.J., Butterfield, M., Fisher, J., Juster, N.P., Watterson, K., Davies, G.A., 1993. Geometry of homograft valve leaflets - effect of dilation of the aorta and the aortic root. Ann. Thorac. Surg. 56, 125–130.

Lu, X., Pandit, A., Kassab, G.S., 2004. Biaxial incremental homeostatic elastic moduli of coronary artery: two-layer model. Am. J. Physiol. Heart Circ. Physiol. 287, H1663–H1669. http://dx.doi.org/10.1152/ajpheart.00226.2004.

Luo, J., Korossis, S.A., Wilshaw, S.P., Jennings, L.M., Fisher, J., Ingham, E., 2014. Development and characterization of acellular porcine pulmonary valve scaffolds for tissue engineering. Tissue Eng. Part A 20, 2963–2974. http://dx.doi.org/10.1089/ten.tea.2013.0573.

Maganti, K., Rigolin, V.H., Sarano, M.E., Bonow, R.O., 2010. Valvular heart disease: diagnosis and management. Mayo Clin. Proc. 85, 483–500. http://dx.doi.org/10.4065/mcp.2009.0706.

Paniagua Gutierrez, J.R., Berry, H., Korossis, S., Mirsadraee, S., Lopes, S.V., da Costa, F., Kearney, J., Watterson, K., Fisher, J., Ingham, E., 2015. Regenerative potential of low-concentration SDS-decellularized porcine aortic valved conduits in vivo. Tissue Eng. Part A 21, 332–342. http://dx.doi.org/10.1089/ten.TEA.2014.0003.

Park, S., Hwang, H.Y., Kim, K.-H., Kim, K.-B., Ahn, H., 2012. Midterm follow-up after cryopreserved homograft replacement in the aortic position. Korean J. Thorac.

Cardiovasc. Surg. 45, 30–34. http://dx.doi.org/10.5090/kjtcs.2012.45.1.30.
Reimer, J.M., Syedain, Z.H., Haynie, B.H.T., Tranquillo, R.T., 2015. Pediatric tubular pulmonary heart valve from decellularized engineered tissue tubes. Biomaterials 62, 88–94. http://dx.doi.org/10.1016/j.biomaterials.2015.05.009.
Rieder, E., Kasimir, M.T., Silberhumer, G., Seebacher, G., Wolner, E., Simon, P., Weigel, G., 2004. Decellularization protocols of porcine heart valves differ importantly in efficiency of cell removal and susceptibility of the matrix to recellularization with human vascular cells. J. Thorac. Cardiovasc. Surg. 127, 399–405. http://dx.doi.org/10.1016/j.jtcvs.2003.06.017.
Roudaut, R., Serri, K., Lafitte, S., 2007. Valve disease - thrombosis of prosthetic heart valves: diagnosis and therapeutic considerations. Heart 93, 137–142. http://dx.doi.org/10.1136/hrt.2005.071183.
Ryan, W.H., Herbert, M.A., Dewey, T.M., Agarwal, S., Ryan, A.L., Prince, S.L., Mack, M.J., 2006. The occurrence of postoperative pulmonary homograft stenosis in adult patients undergoing the Ross procedure. J. Heart Valve Dis. 15, 108–113.
Sabbah, H.N., Hamid, M.S., Stein, P.D., 1986. Mechanical stresses on closed cusps of porcine bioprosthetic valves - correlation with sites of calcification. Ann. Thorac. Surg. 42, 93–96.
Sacks, M.S., Yoganathan, A.P., 2007. Heart valve function: a biomechanical perspective. Philos. Trans. R. Soc. B-Biol. Sci. 362, 1369–1391. http://dx.doi.org/10.1098/rstb.2007.2122.
Sacks, M.S., Schoen, F.J., Mayer, J.E., 2009a. Bioengineering challenges for heart valve tissue engineering. Annu. Rev. Biomed. Eng. 11, 289–313. http://dx.doi.org/10.1146/annurev-bioeng-061008-124903.
Sacks, M.S., Merryman, W.D., Schmidt, D.E., 2009b. On the biomechanics of heart valve function. J. Biomech. 42, 1804–1824. http://dx.doi.org/10.1016/j.jbiomech.2009.05.015.
Schenke-Layland, K., Opitz, F., Gross, M., Doring, C., Halbhuber, K.J., Schirrmeister, F., Wahlers, T., Stock, U.A., 2003. Complete dynamic repopulation of decellularized heart valves by application of defined physical signals - an in vitro study. Cardiovasc. Res. 60, 497–509. http://dx.doi.org/10.1016/j.cardiores.2003.09.002.
Schneider, C.A., Rasband, W.S., Eliceiri, K.W., 2012. NIH Image to ImageJ: 25 years of image analysis. Nat. Methods 9, 671–675. http://dx.doi.org/10.1038/nmeth.2089.
Shaddy, R.E., Hawkins, J.A., 2002. Immunology and failure of valved allografts in children. Ann. Thorac. Surg. 74, 1271–1275. http://dx.doi.org/10.1016/s0003-4975(02)03885-7.
Spina, M., Ortolani, F., El Messlemani, A., Gandaglia, A., Bujan, J., Garcia-Honduvilla, N., Vesely, I., Gerosa, G., Casarotto, D., Petrelli, L., Marchini, M., 2003. Isolation of intact aortic valve scaffolds for heart-valve bioprostheses: extracellular matrix structure, prevention from calcification, and cell repopulation features. J. Biomed. Mater. Res. Part A 67A, 1338–1350. http://dx.doi.org/10.1002/jbm.a.20025.
Syedain, Z.H., Meier, L.A., Reimer, J.M., Tranquillo, R.T., 2013. Tubular heart valves from decellularized engineered tissue. Ann. Biomed. Eng. 41, 2645–2654. http://dx.doi.org/10.1007/s10439-013-0872-9.
Tudorache, I., Cebotari, S., Sturz, G., Kirsch, L., Hurschler, C., Hilfiker, A., Haverich, A., Lichtenberg, A., 2007. Tissue engineering of heart valves: biomechanical and morphological properties of decellularized heart valves. J. Heart Valve Dis. 16, 567–573.
Tudorache, I., Horke, A., Cebotari, S., Sarikouch, S., Boethig, D., Breymann, T., Beerbaum, P., Bertram, H., Westhoff-Bleck, M., Theodoridis, K., Bobylev, D., Cheptanaru, E., Ciubotaru, A., Haverich, A., 2016. Decellularized aortic homografts for aortic valve and aorta ascendens replacement. Eur. J. Cardio-Thorac. Surg. 50, 89–97. http://dx.doi.org/10.1093/ejcts/ezw013.
Vafaee, T., Thomas, D., Desai, A., Jennings, L.M., Berry, H., Rooney, P., Kearney, J., Fisher, J., Ingham, E., 2016. Decellularization of human donor aortic and pulmonary valved conduits using low concentration sodium dodecyl sulfate. J. Tissue Eng. Regen. Med. http://dx.doi.org/10.1002/term.2391.
Walraevens, J., Willaert, B., De Win, G., Ranftl, A., De Schutter, J., Sloten, J.V., 2008. Correlation between compression, tensile and tearing tests on healthy and calcified aortic tissues. Med. Eng. Phys. 30, 1098–1104. http://dx.doi.org/10.1016/j.medengphy.2008.01.006.
Wells, W.J., Arroyo, H., Bremner, R.M., Wood, J., Starnes, V.A., 2002. Homograft conduit failure in infants is not due to somatic outgrowth. J. Thorac. Cardiovasc. Surg. 124, 88–96. http://dx.doi.org/10.1067/mtc.2002.121158.
Wilcox, H.E., Korossis, S.A., Booth, C., Watterson, K.G., Kearney, J.N., Fisher, J., Ingham, E., 2005. Biocompatibility and recellularization potential of an acellular porcine heart valve matrix. J. Heart Valve Dis. 14, 228–237.
Williams, C., Liao, J., Joyce, E.M., Wang, B., Leach, J.B., Sacks, M.S., Wong, J.Y., 2009. Altered structural and mechanical properties in decellularized rabbit carotid arteries. Acta Biomater. 5, 993–1005. http://dx.doi.org/10.1016/j.actbio.2008.11.028.
Zehr, K.J., Yagubyan, M., Connolly, H.M., Nelson, S.M., Schaff, H.V., 2005. Aortic root replacement with a novel decellularized cryopreserved aortic homograft: postoperative immunoreactivity and early results. J. Thorac. Cardiovasc. Surg. 130, 1010–1015. http://dx.doi.org/10.1016/j.jtcvs.2005.03.044.